

Available online at www.sciencedirect.com

ScienceDirect

journal homepage: www.e-jds.com

Original Article

Three-dimensional analysis of coronal root canal morphology of 136 permanent mandibular first molars by micro-computed tomography

Yujie Fu ^{a,b,c}, Yuan Gao ^{a,c}, Yuxuan Gao ^{a,c}, Xuelian Tan ^{a,c},
Lan Zhang ^{a,c}, Dingming Huang ^{a,c*}

^a State Key Laboratory of Oral Diseases & National Clinical Research Centre for Oral Diseases, West China Hospital of Stomatology, Sichuan University, Chengdu, China

^b Department of Endodontics, School and Hospital of Stomatology, Tongji University, Shanghai Engineering Research Centre of Tooth Restoration and Regeneration, Shanghai, China

^c Department of Conservative Dentistry and Endodontics, West China Hospital of Stomatology, Sichuan University, Chengdu, China

Received 11 July 2021; Final revision received 25 July 2021

Available online 13 August 2021

KEYWORDS

Canal curvature;
Micro-computed tomography;
Mandibular first molar;
Modern endodontic access;
Root and canal anatomy;
Three-dimensional reconstruction

Background/purpose: Minimally invasive endodontic approach become a research hotspot and may prevent the fracture of endodontically-treated teeth. This research aims to measure the coronal root canal morphology of permanent mandibular first molars in 3D and propose a new minimally invasive endodontic approach based on this measurement.

Materials and methods: Data of 136 permanent mandibular first molars were involved and re-constructed in 3D models with canals. Then, the morphology characteristics of the coronal root canal were measured.

Results: Overall, the distribution of root canal orifices was more centralized than other landmarks. The landmarks were located more mesiobuccally to the center of the occlusal plane of molars. Specifically, the measurements of the maximum curvature of coronal root canals in the axial direction were: in 3-canals 2-rooted teeth, the average angles of curvatures were 23°, 25°, 11° for mesiobuccal (MB), mesiolingual (ML) and distobuccal (DB) canals, respectively; in 4-canals 2-rooted teeth were 23°, 25°, 12°, 16° for MB, ML, DB, and distolingual (DL) canals, respectively; in 4-canals 3-rooted teeth were 25°, 27°, 17°, 39° for MB, ML, DB, and DL canals, respectively. The degrees of coronal root canal curvatures in the horizontal direction were: in 3-canals teeth, the average angles of curvatures were -1°, 47°, -2° for MB, ML and DB canals,

* Corresponding author. State Key Laboratory of Oral Diseases & National Clinical Research Centre for Oral Diseases & Department of Conservative Dentistry and Endodontics West China Hospital of Stomatology, Sichuan University, 14# 3rd Section, Renmin South Road, Chengdu, Sichuan Province 610041, China.

E-mail address: dingminghuang@163.com (D. Huang).

<https://doi.org/10.1016/j.jds.2021.07.021>

1991-7902/© 2021 Association for Dental Sciences of the Republic of China. Publishing services by Elsevier B.V. This is an open access article under the CC BY-NC-ND license (<http://creativecommons.org/licenses/by-nc-nd/4.0/>).

respectively; in 4-canals 2-rooted teeth were -4° , 41° , -25° , 48° for MB, ML, DB, and DL canals, respectively; in 4-canals 3-rooted teeth were -3° , 33° , -43° , 79° for MB, ML, DB, and DL canals, respectively.

Conclusion: The results of this study are similar to those previously obtained using CBCT and can help us design endodontic approaches.

© 2021 Association for Dental Sciences of the Republic of China. Publishing services by Elsevier B.V. This is an open access article under the CC BY-NC-ND license (<http://creativecommons.org/licenses/by-nc-nd/4.0/>).

Introduction

Recently, the concept of minimally invasive endodontics theory has emerged to promote treatments that prevent the fracture of endodontically-treated teeth.¹ One of the most interesting topics in minimally invasive endodontic therapy is the minimally invasive endodontic approaches. One such approach is conservative endodontic cavities (CEC), first proposed by Clark and Khademi in 2010. CEC minimizes the removal of tooth structure especially so that the pericervical dentine (PCD) can be preserved.² The pericervical dentine is the dentine located in the 4 mm coronal and apical to the crestal bone. Some studies have shown that pericervical dentine plays an important biomechanical function,^{3–5} and its retention can increase the resistance of teeth to fracture.^{5,6} Therefore, a variety of minimally invasive endodontic approaches have been developed with the purpose of preserving more dental tissue, especially pericervical dentin, to prevent the fracture of teeth. However, whether the minimally invasive endodontic approaches can improve the fracture resistance of endodontically-treated teeth is still controversial.^{6–11} In addition, the reduction in the size of the endodontic cavities in CEC reduces the efficiency of root canal shaping and cleaning while such reduction increases the difficulty of treatment.^{12–15}

At present, the lack of knowledge of coronal root canal morphology may be one of the important reasons for the unsatisfactory design of minimally invasive endodontic approaches. Successful root canal therapy depends on a thorough understanding of the anatomy of the root canal system. The mandibular first permanent molar is a frequently treated tooth,¹⁶ and there are numerous studies on its root canal anatomy.^{17–23} These studies provide a solid foundation for more efficient approaches of conventional root canal therapy. Similarly, a successful minimally invasive endodontic approach depends on a thorough understanding of coronal root canal morphology. Unfortunately, past research has not paid much attention to the coronal root canal morphology. This is because a large amount of coronal tooth tissue is removed, thereby eliminating the natural morphology of the coronal root canal, in the process of establishing a straight path in traditional endodontic cavities.

To bridge this gap in knowledge, our research group has previously used cone beam computed tomography (CBCT) data *in vivo* to study coronal root canal morphology of permanent two-rooted mandibular first molars with novel 3D measurement methods.²⁴ The study provided significant

preliminary *in vivo* results, and these results enabled us to make further *in vitro* examinations using micro-computed tomographic (micro-CT) imaging.

Micro-CT imaging is one of the most used methods to study the morphology of the root canal system. Because it provides high resolution 3d imaging and causes no damage to the sample, micro-CT has become the gold standard in root canal morphology research,^{25–27} as mentioned above. With micro-CT, more accurate morphology data can be collected. Importantly, micro-CT does not require manually segmenting the mandibular molars from the tomography images, so we can increase the sample size and include the teeth with radix entomolaris that are relatively common in the Chinese population.^{17,28}

Therefore, the current study aims to determine the landmark location and coronal curvatures of the canal of mandibular first permanent molars by reconstructing them in 3D models using *in vitro* micro-CT images to provide more accurate 3D data. In addition, the combination of *in vivo* results and the current higher-accuracy *in vitro* results enables us to present our novel protocol for minimally invasive endodontic approach.²⁴

Materials and methods

Subjects

This study was approved by the ethics committee of the West China College of Stomatology (WCHSIRB-D-2018-132). Mandibular first molars from a Chinese population that extracted for orthodontic treatment, periodontal treatment or other treatment needs were collected. These teeth were ultrasonically cleaned and maintained in 0.1% thymol solution at 4 °C until use.

The teeth were scanned in a micro-CT system (μ CT-50; Scanco Medical, Bassersdorf, Switzerland) in 90kV/88 μ A with an isotropic voxel size of 30 μ m. Scanning was performed by 500 projections per 180°, camera exposure time of 500 ms. Scanning data were converted to the Digital Imaging and Communication in Medicine (DICOM) format for subsequent analysis.

A total 136 mandibular first permanent molars were included, meeting the following inclusion criteria: (1) the mandibular first permanent molars had fully formed apices; (2) the mandibular first permanent molars had sound coronal structures without root canal fillings, posts, prosthetic crowns, bridges, restorations, caries, trauma, attrition or any other defects.

Measurement in 3D

Micro-CT data were imported into Mimics 18.0 software (Materialise, Leuven, Belgium). The 3-dimensional models of the teeth with root canal system were constructed and made transparent by adjusting the transparency. The tooth axes based on the shape of the tooth was calculated automatically based on principal component analysis (PCA).²⁹

The landmarks were marked directly on the constructed 3D models, and the middle axis of the coronal part of the root canals is obtained: (1) canal orifice point (O): the center point of each root canal at the level of cemento enamel-junction (CEJ); (2) primary curve point (PC): the center of the canal primary curve in the maximum curvature view; (3) the middle axis of the coronal part of the root canals: the straight line connecting O and PC; (4) The intersection point of occlusal surface (IO): the intersection point between the middle axis of the coronal part of the root canals and the occlusal surface (Fig. 1A).

The occlusal view screenshots of models aligned by their teeth axes were taken and transferred into image processing software (Adobe Photoshop CC 2017.0.0; Adobe Inc., San Jose, CA, USA). Then a 32×32 -grid analytical plane was fitted on each screenshot. The direction of x-axes of the planes were along mesiodistal axes of the tooth crowns and y-axes were along buccolingual axes of the tooth crowns. On the x-axis, "1" and "32" represent the mesial end and the distal end, respectively. On the y-axis, "1" and "32" represent the buccal end and the lingual end, respectively. The coordinates of the landmarks were recorded (Fig. 1B).

The occlusal view screenshots of models with analytical plane were imported into ImageJ 1.51K software (National

Institutes of Health, Bethesda, MD, USA) for measurements of curvature direction in the horizontal direction, which is the angle formed by x-axes of analytical planes and the middle axes of the coronal part of the root canal (Fig. 1C). The angle was recorded as negative when the middle axis tended to the side of the lingual side.

The angle formed by the middle axes of the coronal part of the root canal and teeth axes is coronal root canal curvature in the axial direction. In the Mimics Research 18.0 software, a straight line parallel to the tooth axis was made through the PC point in the maximum curvature view, and the angle measurement tool in the software was used to measure the angle.

Statistical analysis

The coronal root canal curvature of the occlusal and axial aspect between different root canals were analyzed. Statistically significant differences about the coronal root canal curvature in the axial direction among canals were evaluated using the Friedman test and Dunn's multiple comparisons test with Prism GraphPad 7.0 (GraphPad Software, La Jolla, CA, USA), with significance level (alpha level) set at 0.05. The coordinates of landmarks were analyzed by spatial statistics methods.³⁰

Results

Distribution of landmarks in occlusal aspect

The distribution characteristics of landmarks in the mandibular first molars are presented in Table 1. The distribution maps of landmarks are presented in Fig. 2.

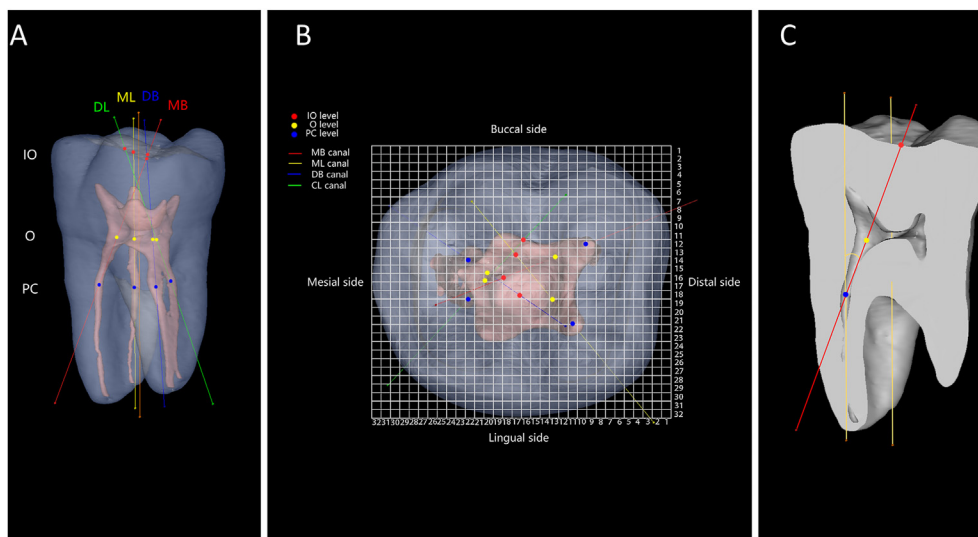


Figure 1 Schematic diagram of 3D measurement method. (A) A three-dimensional model constructed from micro-CT data showing selected landmarks: the centre of each canal orifice (O) at the level of cemento enamel-junction (CEJ), the centre of the canal primary curve (PC) in the maximum curvature view and the intersection point of the middle axis of the coronal part of the root canal and the occlusal surface (IO). (B) View from the occlusal aspect of a mandibular first molar with a 32×32 -grid (C) Three-dimensional model of CBCT data showing the determination of the maximum angle of curvature in the maximum coronal root canal curvature in the axial direction.

Table 1 The distribution characteristics of landmarks according to number of canals.

		Mean Centre			Standard Distance		
		O	PC	IO	O	PC	IO
3 Canals (2 roots)	MB	(10.95,14.80)	(6.08,14.81)	(17.25,14.59)	1.10	1.63	1.65
	ML	(11.69,19.53)	(7.67,23.14)	(16.98,14.86)	1.25	1.96	2.21
	D	(18.92,16.64)	(20.95,16.77)	(15.84,16.38)	0.88	1.22	1.59
4 Canals (2 roots)	MB	(10.56,14.40)	(6.04,14.04)	(17.08,14.96)	0.90	2.35	1.46
	ML	(11.68,19.84)	(7.40,23.84)	(17.28,14.40)	1.18	1.83	2.38
	DB	(18.16,15.16)	(20.24,14.04)	(14.96,16.96)	0.92	1.47	1.84
4 Canals (3 roots)	DL	(18.92,18.00)	(20.92,20.64)	(15.28,13.96)	1.23	1.72	2.78
	MB	(10.59,14.04)	(5.30,13.76)	(17.48,14.33)	0.89	1.51	1.49
	ML	(11.65,19.24)	(6.63,22.65)	(17.87,14.80)	1.24	1.69	1.98
	DB	(17.89,15.07)	(20.43,12.41)	(14.00,18.93)	0.87	1.39	2.12
	DL	(18.70,19.85)	(20.46,30.35)	(16.30,6.48)	1.17	1.89	2.37

D, single distal canal in the distal root; DB, distobuccal; DL, distolingual; MB, mesiobuccal; ML, mesiolingual; O, the centre of each canal orifice; PC, the centre of the canal primary curve; IO, the intersection point of the middle axis of the coronal part of the root canal and the occlusal surface. Mean Centre identifies the geographic centre for a set of coordinates and is a point constructed from the average x and y values for set of coordinates (where x_i and y_i are the coordinates for point "i", represents the Mean Centre for the points, and n is equal to the total number of points). The specific formula is $(\bar{x} = \sum_{i=1}^n x_i \cdot \frac{1}{n}, \bar{y} = \sum_{i=1}^n y_i \cdot \frac{1}{n})$

Standard Distance (SD) measures the degree to which points are concentrated or dispersed around the geometric mean centre. The specific calculation formula is $SD = \sqrt{\sum_{i=1}^n (x_i - \bar{x})^2 \cdot \frac{1}{n} + \sum_{i=1}^n (y_i - \bar{y})^2 \cdot \frac{1}{n}}$.

Standard Distance (SD) measures the degree to which points are concentrated or dispersed around the geometric mean centre. The specific calculation formula is $SD = \sqrt{\sum_{i=1}^n (x_i - \bar{x})^2 \cdot \frac{1}{n} + \sum_{i=1}^n (y_i - \bar{y})^2 \cdot \frac{1}{n}}$.

Among the standard distance values of O, PC and IO, the standard distance values of O point are relatively small, indicating that the distribution of O point is relatively concentrated, while IO and PC are relatively discrete.

By comparing the distribution of landmarks between the two-rooted first mandibular molars with three canals, the two-rooted mandibular first molars with four canals and the three-rooted mandibular first molars with four canals, the distribution of O, PC and IO of mesiobuccal (MB) and mesiolingual (ML) root canals was relatively consistent. The distribution of O and PC of the distolingual (DL) root canal was more inclined to the lingual side when there were radix entomolaris among the mandibular first molars with four canals.

The standard distance values for the O, PC and IO points were all small. The standard distance value of O points was relatively smallest among the three, suggesting that the distribution of O points were relatively concentrated, while IO and PC points were relatively discrete.

The coronal root canal curvature in the axial direction

The degrees of coronal root canal curvature in the axial direction are: in two-rooted the first mandibular molars with three canals, the average angles of curvatures were 23° for the MB, 25° for ML and 11° for the distal canal; in the two-rooted mandibular first molars with four canals, the average angles of curvatures were 23° for the MB, 25° for the ML and 12° for the distobuccal (DB), and 16° for the DL canal; in the three-rooted mandibular first molars with four canals, the average angles of curvatures were 25° for the MB, 27° for the ML and 17° for the DB, and 39° for the DL canal. The degrees of coronal root canal curvature in the axial direction are summarized in [Table 2](#).

In two-rooted the first mandibular molars with three canals, the degree of curvature in the distal root canals were significantly smaller than that in the MB and ML root canals in the axial direction ($p < 0.05$). There was no statistically significant difference in the degree of curvature between ML and MB root canals ($p > 0.05$). In the two-rooted mandibular first molars with four canals, the degree of curvature in the axial direction was significantly smaller in the DB root canals than in the MB root canals ($p < 0.05$), was significantly smaller in the DL root canals than in the ML root canals ($p < 0.05$) and was smaller in the DB root canals than in the DL root canals ($p < 0.05$). There was no statistically significant difference in the degree of curvature between ML and MB root canals ($p > 0.05$). In the three-rooted mandibular first molars with four canals, the degree of curvature in the axial direction was largest in the DL root canals and the smallest in the DB root canals among all root canals ($p < 0.05$), and there was no significant difference between the ML and MB root canals ($p > 0.05$).

Curvature direction of coronal root canal in the horizontal direction

All mesial root canals pointed in the distal direction and vice versa for distal root canals. The degrees of curvature direction of coronal root canal in the horizontal direction are: in two-rooted the first mandibular molars with three canals, the average angles of curvatures were -1° for the MB, 47° for the ML and -2° for the distal canal; in the two-rooted mandibular first molars with four canals, the average angles of curvatures were -4° for the MB, 41° for the ML and -25° for the DB, and 48° for the DL canal; in the three-rooted mandibular first molars with four canals, the average angles of curvatures were -3° for the MB, 33° for

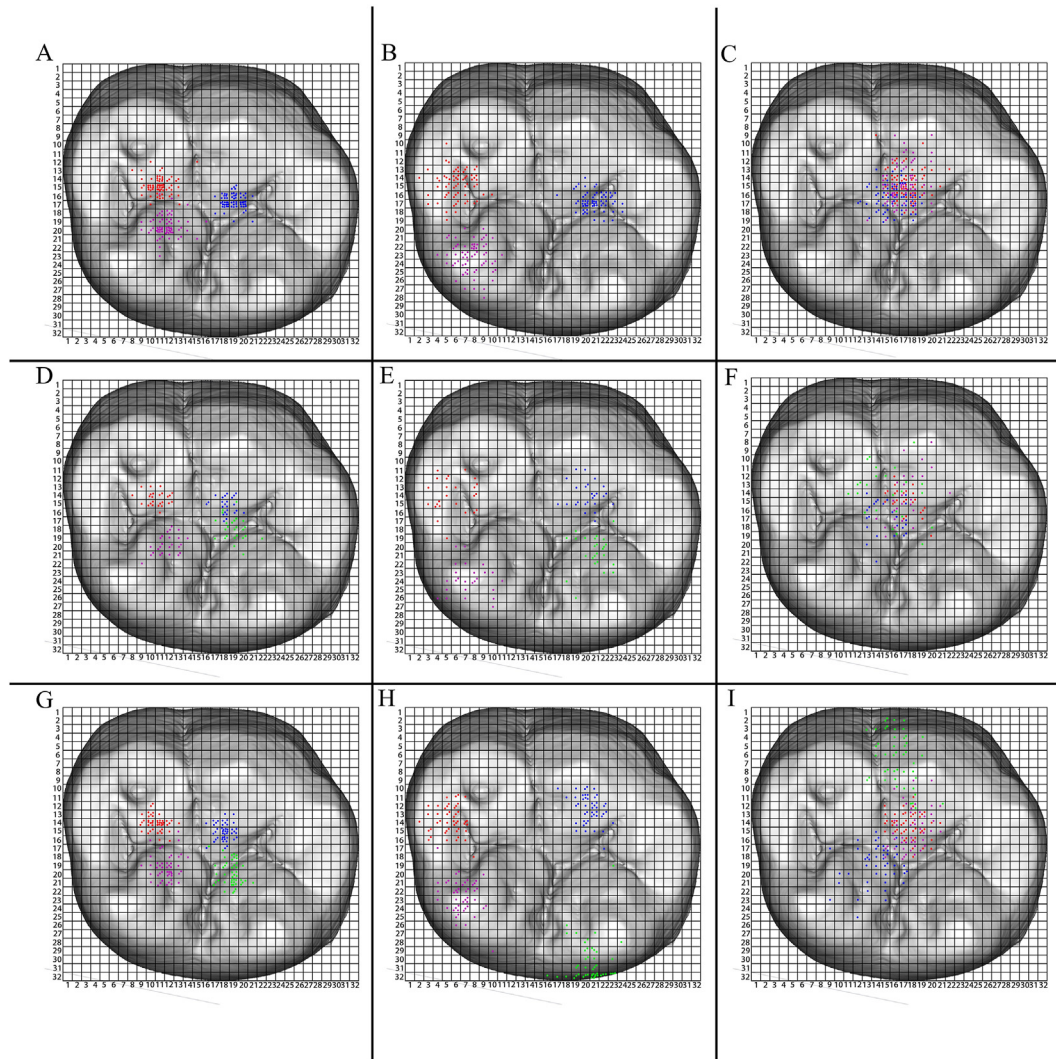


Figure 2 The distribution maps of landmarks. Red dots represent MB landmarks, Purple dots ML landmarks, Blue dots the DB or D landmarks and Green dots the DL landmarks. (A) Root canal orifices in 2-rooted 3-canals, (B) centre of the canal primary curve in 2-rooted 3-canals, (C) intersection point of occlusal surface in 2-rooted 3-canals, (D) root canal orifices in 2-rooted 4-canals, (E) centre of the canal primary curve in 2-rooted 4-canals, (F) intersection point of occlusal surface in 2-rooted 4-canals. (G) Root canal orifices in 3-rooted 4-canals, (H) centre of the canal primary curve in 3-rooted 4-canals, (I) intersection point of occlusal surface in 3-rooted 4-canals.

the ML and -43° for the DB, and 79° for the DL canal. The angles of coronal root canal curvature in the axial direction summarized in [Table 3](#).

Discussion

The *in vitro* 3D measurements collected in this experiment was largely consistent with the *in vivo* measurements reported in our previous study,²⁴ with the only major difference being that the equipment for image scanning switched from CBCT to micro-CT. In root canal morphology studies, micro-CT has the advantage of higher imaging resolution compared with CBCT.^{31–33} In addition, compared with the previous CBCT study, the micro-CT methods in the current study directly scanned the extracted teeth, eliminating the need for complex image steps of segmentation, improving the efficiency of the study and helping to increase the

sample size. Compared to the previous study, in terms of the distribution of landmarks in occlusal aspect, there is little difference in the location of the average centers of landmarks, but the standard distance of landmarks was reduced. The reason for this discrepancy may be due to the higher accuracy of the micro-CT data and the relatively larger sample size in this study. In terms of the coronal root canal curvature in the axial direction and curvature direction of coronal root canal in the horizontal direction, the results of the present study are also in general agreement with the trend of previous results in two-rooted mandibular first molars.

The distolingual root (radix entomolaris) is an anatomical variant commonly found in mandibular first molars in Chinese population.^{17,28} The occurrence of radix entomolaris often makes the treatment of mandibular first molars more difficult because the distal lingual root canal is more

Table 2 Angle of coronal root canal curvature in the axial direction (degrees).

	n	Mean	SD	MIN	MAX	M
3 Canals						
(2 roots)						
MB	65	22.62	4.49	12.84	30.92	22.69
ML	65	24.92	4.30	9.69	37.09	24.93
D	65	10.53	3.81	2.16	18.07	11.14
4 Canals						
(2 roots)						
MB	25	22.50	4.27	15.22	33.54	22.74
ML	25	24.69	4.14	15.67	33.20	23.51
DB	25	12.16	4.19	2.89	17.58	13.35
DL	25	16.20	6.15	4.83	29.82	18.08
4 Canals						
(3 roots)						
MB	46	24.53	4.27	16.31	34.19	24.59
ML	46	26.54	3.97	16.98	37.94	26.21
DB	46	16.57	3.63	10.57	25.62	16.24
DL	46	38.72	7.23	25.34	54.92	37.90

D, single distal canal in the distal root; DB, distobuccal; DL, distolingual; MB, mesiobuccal; ML, mesiolingual; SD, standard deviation; MIN, minimum value; MAX, maximum value; M, median.

Table 3 Angle of curvature direction of coronal root canal in the horizontal direction (degrees).

	n	Mean	SD	MIN	MAX	M	TB (n)	TL (n)
3 Canals								
(2 roots)								
MB	65	-0.8	14.51	-60.91	32.14	0.01	33	32
ML	65	46.59	12.10	15.53	69.87	48.92	65	0
D	65	-1.55	12.29	-23.78	28.93	-2.48	36	29
4 Canals								
(2 roots)								
MB	25	-3.91	12.00	-30.92	14.48	-0.71	10	15
ML	25	41.28	12.03	18.84	59.78	41.98	25	0
DB	25	-24.47	27.30	-73.99	18.87	-19.84	5	20
DL	25	47.72	20.99	19.06	85.03	48.37	25	0
4 Canals								
(3 roots)								
MB	46	-2.77	10.54	-25.89	20.05	-3.58	28	18
ML	46	32.60	11.42	5.21	70.63	33.54	46	0
DB	46	-43.33	18.23	-78.82	-6.12	-41.11	0	46
DL	46	79.38	5.92	59.14	90.00	80.42	46	0

D, single distal canal in the distal root; DB, distobuccal; DL, distolingual; MB, mesiobuccal; ML, mesiolingual; SD, standard deviation; MIN, minimum value; MAX, maximum value; M, median; TB, to buccal direction; TL, to lingual direction.

The angle is recorded as negative when the middle axis tends to the side of the lingual side.

easily missed and has a greater curvature and smaller canal diameter.^{34–37} Familiarity with the relevant morphology features is an important key to successful treatment. Thus, in this study, we also performed measurements on mandibular first molars with radix entomolaris which were

not included in our previous study. Compared with the two-rooted mandibular first molars with four canals, DL root canal orifices of three-rooted mandibular first molars were more lingually oriented. This suggests that we should look more lingually towards the distolingual root canal orifice in the presence of the radix entomolaris, consistent with existing reports.³⁸ Furthermore, there were greater coronal root canal curvatures in the axial direction in the DL canal of mandibular first molars with radix entomolaris. As we mentioned by Fu et al.,²⁴ the curvature of the coronal part of the root canal may be used to evaluate the additional difficulty in root canal preparation in conservative endodontic cavities compared with that in traditional endodontic access cavities. Greater curvature suggests that there may be additional difficulty. In the presence of a radix entomolaris, we recommend careful scrutiny when considering a minimally invasive access preparation of the affected tooth, because such a preparation may increase the difficulty of the treatment and compromise the outcome. Due to the coronal root canal curvature in the axial direction, it is recommended that a more sufficient straight line access be established during the preparation of the DL root canal of the mandibular first molar with the radix entomolaris to help reduce the deformation of the instruments in the root canal and to reduce the pressure of the instruments on the lateral wall of the root canal as well as the stress on the instruments themselves to avoid complications of root canal treatment such as perforation, step and instrument separation.^{24,34–37}

The results of this study are consistent with the results of previous studies, suggesting that *in vivo* CBCT for morphology studies of coronal root canal can indeed meet the corresponding accuracy requirements and that the use of CBCT as an evaluation tool in subsequent minimally invasive access clinical studies may be a reliable option.

Although Micro-CT cannot be used directly in clinical practice due to high radiation doses, its higher accuracy can help us better understand the coronal root canal morphology. With the recent rapid development of deep learning technology,^{39,40} the accurate data from micro-CT is expected to be used to assist in improving the accuracy of CBCT based measurement, and thus the accuracy of minimally invasive approach planning.

In addition, since micro-CT is more accurate compared to CBCT,^{31–33} based on the results of this study, we also present our proposal for a minimally invasive endodontic approach design: straight-line minimally invasive endodontics access cavities (SMEC) (Fig. 3). The preparation of SMEC begins in the central fossa, with a small portion of the roof of the chamber removed, the extent of cavity is controlled so that the canal orifice is not visible from the occlusal view. Afterwards, the cavity shape was expanded according to the direction of the mean central coordinates of the root canal orifice in the present study, with limited straight-line access localized at the coronal side of the root canal of the mesial root canals in two-rooted teeth and the mesial root canals and distolingual root canal in three-rooted teeth. According to our 3-dimensional analysis of coronal root canal morphology of mandibular first molars, the SMEC was designed with the root canal orifice as the key marker point since the distribution of root canal orifices is the most constant. In contrast to CEC, we have innovatively

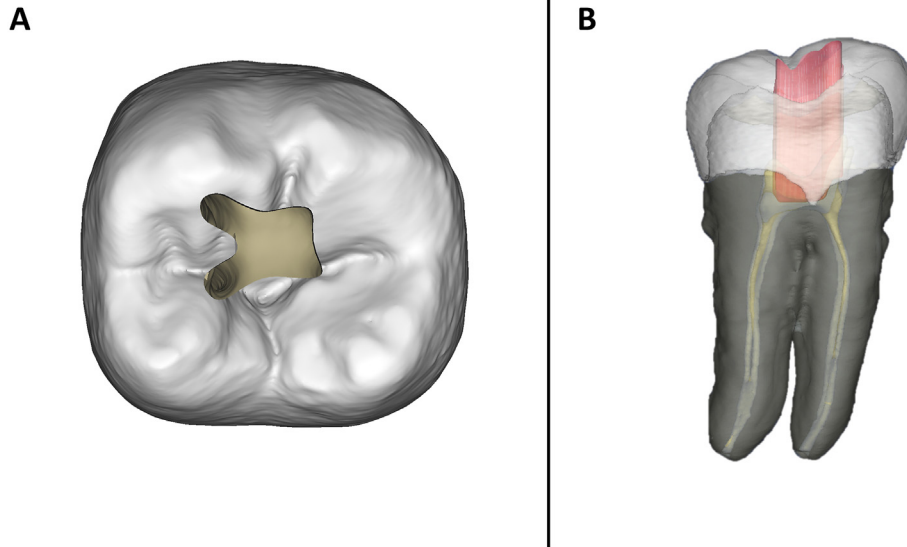


Figure 3 An illustration of the straight-line minimally invasive endodontics access cavities. (A) Occlusal view, (B) buccal view: the red zone represents the access.

introduced a limited straight-line pathway in SMEC. The SMEC requires the establishment of a locally limited straight-line pathway to remove only a portion of the PCD from the coronal side of the root canal with a greater coronal root canal curvature in the axial direction which, according to the results of this study, is the MB and ML root canal of all types of mandibular first molars and the DL root canal of mandibular first molars with radix entomolaris. As a result, limited straight-line access provides better visualization and reduces instrument curvature in the root canal during preparation, with only a small increase in PCD loss. The SMEC was designed based on both root canal morphology studies and biomechanical considerations, and it is hoped that its effectiveness can be demonstrated in subsequent studies.

Declaration of competing interest

The authors have no conflicts of interest relevant to this article.

Acknowledgments

This work was supported by the National Natural Science Foundation of China (No. 81970936 to [D.M.H]), Key Research and Development Program of Sichuan province (No. 2021YFS0031 to [D.M.H]). The authors deny any conflicts of interest related to this study.

References

1. Gluskin AH, Peters CI, Peters OA. Minimally invasive endodontics: challenging prevailing paradigms. *Br Dent J* 2014;216:347–53.
2. Clark D, Khademi J. Modern molar endodontic access and directed dentin conservation. *Dent Clin* 2010;54:249–73.
3. Palamara JEA, Palamara D, Messer HH. Strains in the marginal ridge during occlusal loading. *Aust Dent J* 2002;47:218–22.
4. Merdji A, Mootanah R, Bachir Bouiadjra BA, et al. Stress analysis in single molar tooth. *Mater Sci Eng C Mater Biol Appl* 2013;33:691–8.
5. Jiang Q, Huang Y, Tu X, Li Z, He Y, Yang X. Biomechanical properties of first maxillary molars with different endodontic cavities: a finite element analysis. *J Endod* 2018;44:1283–8.
6. Krishan R, Paqué F, Ossareh A, Kishen A, Dao T, Friedman S. Impacts of conservative endodontic cavity on root canal instrumentation efficacy and resistance to fracture assessed in incisors, premolars, and molars. *J Endod* 2014;40:1160–6.
7. Wang Q, Liu Y, Wang Z, et al. Effect of access cavities and canal enlargement on biomechanics of endodontically treated teeth: a finite element analysis. *J Endod* 2020;46:1501–7.
8. Plotino G, Grande NM, Isufi A, et al. Fracture strength of endodontically treated teeth with different access cavity designs. *J Endod* 2017;43:995–1000.
9. Moore B, Verdelis K, Kishen A, Dao T, Friedman S. Impacts of contracted endodontic cavities on instrumentation efficacy and biomechanical responses in maxillary molars. *J Endod* 2016;42:1779–83.
10. Corsentino G, Pedullà E, Castelli L, et al. Influence of access cavity preparation and remaining tooth substance on fracture strength of endodontically treated teeth. *J Endod* 2018;44:1416–21.
11. Özyürek T, Ülker Ö, Demiryürek EÖ, Yılmaz F. The effects of endodontic access cavity preparation design on the fracture strength of endodontically treated teeth: traditional versus conservative preparation. *J Endod* 2018;44:800–5.
12. Augusto CM, Barbosa AFA, Guimarães CC, et al. A laboratory study of the impact of ultraconservative access cavities and minimal root canal tapers on the ability to shape canals in extracted mandibular molars and their fracture resistance. *Int Endod J* 2020;53:1516–29.
13. Vieira GCS, Pérez AR, Alves FRF, et al. Impact of contracted endodontic cavities on root canal disinfection and shaping. *J Endod* 2020;46:655–61.
14. Rover G, Belladonna FG, Bortoluzzi EA, De-Deus G, Silva EJNL, Teixeira CS. Influence of access cavity design on root canal detection, instrumentation efficacy, and fracture resistance assessed in maxillary molars. *J Endod* 2017;43:1657–62.

15. Alovisi M, Pasqualini D, Musso E, et al. Influence of contracted endodontic access on root canal geometry: an in vitro study. *J Endod* 2018;44:614–20.
16. Wayman BE, Patten JA, Dazey SE. Relative frequency of teeth needing endodontic treatment in 3350 consecutive endodontic patients. *J Endod* 1994;20:399–401.
17. Wang Y, Zheng Q-h, Zhou X-d, et al. Evaluation of the root and canal morphology of mandibular first permanent molars in a western Chinese population by cone-beam computed tomography. *J Endod* 2010;36:1786–9.
18. Zhang R, Wang H, Tian YY, Yu X, Hu T, Dummer PMH. Use of cone-beam computed tomography to evaluate root and canal morphology of mandibular molars in Chinese individuals. *Int Endod J* 2011;44:990–9.
19. Keles A, Keskin C. Deviations of mesial root canals of mandibular first molar teeth at the apical third: a micro-computed tomographic study. *J Endod* 2018;44:1030–2.
20. Lee JK, Yoo YJ, Perinpanayagam H, et al. Three-dimensional modelling and concurrent measurements of root anatomy in mandibular first molar mesial roots using micro-computed tomography. *Int Endod J* 2015;48:380–9.
21. Keleş A, Keskin C. Apical root canal morphology of mesial roots of mandibular first molar teeth with vertucci type II configuration by means of micro-computed tomography. *J Endod* 2017;43:481–5.
22. Wolf TG, Paqué F, Zeller M, Willershausen B, Briseño-Marroquín B. Root canal morphology and configuration of 118 mandibular first molars by means of micro-computed tomography: an ex vivo study. *J Endod* 2016;42:610–4.
23. Eaton JA, Clement DJ, Lloyd A, Marchesan MA. Micro-computed tomographic evaluation of the influence of root canal system landmarks on access outline forms and canal curvatures in mandibular molars. *J Endod* 2015;41:1888–91.
24. Fu Y, Deng Q, Xie Z, et al. Coronal root canal morphology of permanent two-rooted mandibular first molars with novel 3D measurements. *Int Endod J* 2020;53:167–75.
25. Lee J-H, Kim K-D, Lee J-K, et al. Mesiobuccal root canal anatomy of Korean maxillary first and second molars by cone-beam computed tomography. *Oral Surg Oral Med Oral Pathol Oral Radiol Endod* 2011;111:785–91.
26. Ordinola-Zapata R, Bramante CM, Versiani MA, et al. Comparative accuracy of the clearing technique, CBCT and micro-CT methods in studying the mesial root canal configuration of mandibular first molars. *Int Endod J* 2017;50:90–6.
27. Briseño-Marroquín B, Paqué F, Maier K, Willershausen B, Wolf TG. Root canal morphology and configuration of 179 maxillary first molars by means of micro-computed tomography: an ex vivo study. *J Endod* 2015;41:2008–13.
28. Huang RY, Cheng WC, Chen CJ, et al. Three-dimensional analysis of the root morphology of mandibular first molars with distolingual roots. *Int Endod J* 2010;43:478–84.
29. Kim G, Lee J, Seo J, Lee W, Shin Y-G, Kim B. Automatic teeth axes calculation for well-aligned teeth using cost profile analysis along teeth center arch. *IEEE Trans Biomed Eng* 2012;59:1145–54.
30. Mitchel A. *The ESRI Guide to GIS analysis, 2. Spatial measurements and statistics*, 2005.
31. Marca C, Dummer PMH, Bryant S, et al. Three-rooted premolar analyzed by high-resolution and cone beam CT. *Clin Oral Invest* 2013;17:1535–40.
32. Zhang D, Chen J, Lan G, et al. The root canal morphology in mandibular first premolars: a comparative evaluation of cone-beam computed tomography and micro-computed tomography. *Clin Oral Invest* 2017;21:1007–12.
33. Tolentino EDS, Amoroso-Silva PA, Alcalde MP, et al. Accuracy of high-resolution small-volume cone-beam computed tomography in detecting complex anatomy of the apical isthmi: ex vivo analysis. *J Endod* 2018;44:1862–6.
34. De Moor RJG, Deroose CAJG, Calberson FLG. The radix entomolaris in mandibular first molars: an endodontic challenge. *Int Endod J* 2004;37:789–99.
35. Gu Y, Lu Q, Wang P, Ni L. Root canal morphology of permanent three-rooted mandibular first molars: Part II-measurement of root canal curvatures. *J Endod* 2010;36:1341–6.
36. Gu Y, Zhou P, Ding Y, Wang P, Ni L. Root canal morphology of permanent three-rooted mandibular first molars: Part III-An odontometric analysis. *J Endod* 2011;37:485–90.
37. Rodrigues CT, Oliveira-Santos Cd, Bernardineli N, et al. Prevalence and morphometric analysis of three-rooted mandibular first molars in a Brazilian subpopulation. *J Appl Oral Sci* 2016;24:535–42.
38. Gu Y, Lu Q, Wang H, Ding Y, Wang P, Ni L. Root canal morphology of permanent three-rooted mandibular first molars-part I: pulp floor and root canal system. *J Endod* 2010;36:990–4.
39. Hiraiwa T, Arijji Y, Fukuda M, et al. A deep-learning artificial intelligence system for assessment of root morphology of the mandibular first molar on panoramic radiography. *Dentomaxillofacial Radiol* 2019;48:20180218.
40. Choe J, Lee SM, Do K-H, et al. Deep learning-based image conversion of CT reconstruction kernels improves radiomics reproducibility for pulmonary nodules or masses. *Radiology* 2019;292:365–73.